Synthesis and Characterization of Low Bandgap Copolymers Based on Indenofluorene and Thiophene Derivative

WEI-CHE YEN,[1] BIKASH PAL,[2,3] JYE-SHANE YANG,[3] YING-CHIEH HUNG,[4] SHIANG-TAI LIN,[4] CHI-YANG CHAO,[2] WEI-FANG SU[1,2]

[1]Institute of Polymer Science and Engineering, National Taiwan University, Taipei, Taiwan

[2]Department of Material Science and Engineering, National Taiwan University, Taipei, Taiwan

[3]Department of Chemistry, National Taiwan University, Taipei, Taiwan

[4]Department of Chemical Engineering, National Taiwan University, Taipei, Taiwan

Received 18 March 2009; accepted 2 June 2009
DOI: 10.1002/pola.23557
Published online in Wiley InterScience (www.interscience.wiley.com).

ABSTRACT: A series of low band gap, highly soluble alternating conjugated copolymers, comprised of 11,11,12,12-tetrahexylindenofluorene and thiophene derivatives (**P1-P4**), were synthesized via Pd-catalyzed Suzuki coupling reaction with very good yields. Described here are the synthesis, thermal, optical, and electrochemical properties of these new copolymers as potential new active materials for electronic and optoelectronic device applications. **P1** and **P2** have electron donating non-π-substituents with ethylenedioxy and propylenedioxy bridging the 3,3 positions of the cyclopentadithiophene groups; whereas **P3** and **P4** have electron withdrawing π-substituents (carbonyl and pyrazine groups on **P3** and **P4**, respectively). For the main absorptions in UV-vis spectrum, **P1** and **P2** displayed more red absorptions in comparison with **P3** and **P4**. Nevertheless, much suppressed quantum yields are exhibited by **P3** and **P4**. The behaviors of **P3** can be attributed to the significant charge transfer interactions between the π-substituents and the conjugated polymer backbone that leads to a less allowed optical transition between the ground and the lowest excited state. For **P4**, the weak fluoresence might associate with energy transfer from indenofluorene to the low band gap thiophene-pyrazinethiophene-thiophene (T-PT-T) unit. In comparison with the corresponding polymers containing fluorene instead of indenofluorene, the use of indenofluorene exhibited mixed effects on the optical properties and improved solubility. © 2009 Wiley Periodicals, Inc. J Polym Sci Part A: Polym Chem 47: 5044–5056, 2009

Keywords: charge transport; conjugated polymers; indenofluorene; meta conjugation effect; metal-organic catalysts/organometallic catalysts; π-substituent

INTRODUCTION

Conjugated polymers have received a great deal of attention for uses in polymer solar cell[1–10] and organic light emitting diodes (OLEDs).[11] Photophysical and electrochemical properties of conjugated copolymers are primarily governed by the

Additional Supporting Information may be found in the online version of this article.

Correspondence to: W.-F. Su (E-mail: suwf@ntu.edu.tw)

Journal of Polymer Science: Part A: Polymer Chemistry, Vol. 47, 5044–5056 (2009)

chemical structures of the polymer backbone. Researches of low band gap conjugated copolymers have been particularly rich in the recent past mainly for their high intrinsic conductivity[12] and potential application on infrared electrochromic displays and solar cells.[13,14] Thiophene-based and cyclopentadithiophene-based copolymers are among the mostly studied low band gap polymer systems.[12,15] Copolymers comprised of fluorene and cyclopentadithiophene derivatives as well as poly(cyclopentadithiophene)s have been used in light absorbing diode due to their high efficient red and infrared absorption properties in solar spectra.[16] In particular, these polymers possess the lowest known band gaps in the range from 0.16 to 1.5 eV.[17–20] However, it is also known that the aforementioned copolymers have some drawbacks such as poor solubility in common organic solvents, excimers formation in the solid state, and low charge transfer mobility. According to our previous work and literatures, alternating copolymers comprised of fluorene and monomers **2–5** (chemical structures shown in Scheme 1) were reported to show limited solubility in common organic solvents.[16,21]

To improve the solubility of fluorene-cyclopentadithiophene copolymers, the incorporation of indenofluorene unit in the polymer backbone to replace fluorene could be an appraisable idea as polyindenofluorene derivatives showed very good solubility due to the presence of four hexyl groups. The enhancement of solubility could be attributed to the effectively suppression of the aggregation of indenofluorene segments.[22,23] In addition, polyindenofluorene derivatives also exhibited very good charge mobility in both neutral and doped states due to its rigid, planar molecular structure, and the longer conjugated *p*-terphenyl moiety.[24] Hence, indenofluorene unit might increase the conjugation length of the corresponding copolymers, leading to optical absorption at longer wavelengths. The combination of monomer **2–5** and indenofluorene derivatives should make the copolymers highly soluble in common organic solvent due to the presence of four hexyl groups at 11,12 position, yet preserve desired optoelectrical properties such as red-shifted absorption, low band gap, good charge mobility in both neutral and doped states.

In this article, we report the synthesis and characterization of four new alternating copolymers **P1**, **P2**, **P3**, and **P4** comprised of indenofluorene and thiophene/cyclopentadithiophene derivatives. The thermal, optical, and electrochemical properties of these four polymers were also investigated. The non-π-substituents in **P1** and **P2** were found to have little effects on the fluorescence quantum efficiency. The electron-withdrawing π-substituents in **P3** and **P4** shown two absorption peaks in UV-vis spectra and lowered the fluorescence quantum yields. The observation of **P3** and **P4** indicated that the presence of charge transfer between the π-substituent and the conjugated polymer backbone could facilitate efficient charge separation for high efficiency solar cell sensitizer.

EXPERIMENTAL

General

Reagents and chemicals were purchased from Aldrich Chemical Co. unless otherwise stated. All the new compounds were characterized by ^{1}H NMR and ^{13}C NMR and FTIR spectra. FTIR spectra were recorded on a Perkin Elmer spectrum 100. NMR spectra were collected on a Bruker AVANCE 400 spectrometers with $CDCl_3$ and DMSO-d_6 as solvent and tetramethyl silane as internal standard. Melting points (M.P.) were measured on a MEL-TEMP II melting point apparatus. Molecular weights of the polymers were determined by gel permeation chromatography (GPC) on a Waters 1525 Binary HPLC Pump with polystyrene as the standard and THF as the solvent. The molecular orbital distributions of polymers were calculated using quantum mechanical package Gaussian 03 and plotted using GaussView program. UV-visible spectra were recorded on a Perkin Elmer Lambda 35 UV/VIS Spectrometer. The photoluminescence (PL) spectra were measured by exciting the polymer samples at 325 nm and the emission was measured with a Perkin Elmer LS 55 Luminescence spectrometer. An integrating sphere made by Labsphere was used to measure the PL efficiencies. Solutions used to detect UV-visible spectra and PL spectra were prepared from the polymer dissolved in THF. UV-visible spectra and PL spectra in the solid state were carried out on films spin-coated onto quartz plate from chloroform solution. Cyclic voltammetry (CV) was performed on a CH Instruments 611B potentiostat/galvanostat system with a three-electrode cell in a solution of Bu_4NPF_6 (0.05 M) in dichloromethane (DCM) with reversible or partly reversible oxidations and in tetrahydrofuran (THF) with reversible or

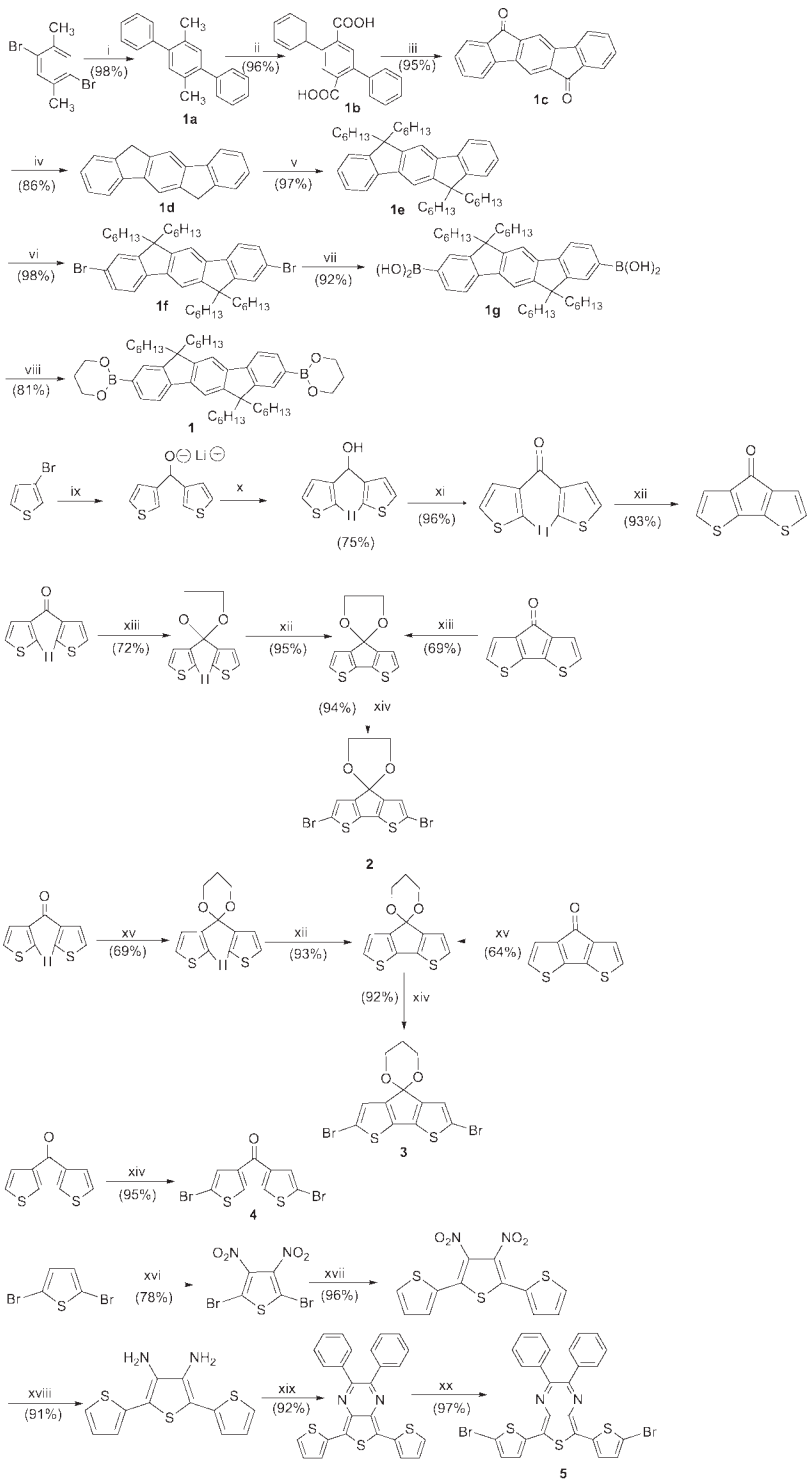

[a]Reagents and Conditions: i.Phenylboronic acid, $Pd(OAc)_2$, K_2CO_3, $(Bu)_4NBr$, H_2O, 70°C, ii. Pyridine, H_2O, $KMnO_4$, Reflux, iii. Conc H_2SO_4, iv. $HOCH_2CH_2OH$, NH_2NH_2. H_2O, KOH, MW, 300W, 150°C, 30min, v. THF, *n*-BuLi, $C_6H_{13}Br$, r.t, vi. $CHCl_3$, $FeCl_3$ (cat.), Br_2(2 eq), vii. THF, *n*-BuLi, (*i*-PrO)$_3$B, -78°C, 2M HCl, viii. Toluene, 1,3-propandiol, Reflux, ix. (a) Ether, *n*-BuLi, -78°C, (b) 3-thiophenecarboxaldehyde, x. (a) *n*-BuLi (2eqiv.), -23°C, I_2 (3eqiv.), (b) Na_2SO_3 and HI solun, xi. CH_2Cl_2, P.C.C, r.t, xii. Cu, DMF, Reflux, xiii. C_6H_6, $HOCH_2CH_2OH$, PTSA (cat.), azeotrope, 110°C, 4 days, xiv. THF, NBS, 0°C, xv. C_6H_6, $HOCH_2CH_2CH_2OH$, PTSA (cat.), azeotrope, 110°C, 4 days, xvi. Conc H_2SO_4, fuming HNO_3, fuming H_2SO_4, xvii. Tributyl(thiophen-2-yl)stannane (2eq), THF, $[Pd(Ph_3)_4]Cl_2$, Reflux, xviii. C_2H_5OH, Conc HCl, Anh. $SnCl_2$, 40°C, xix. MeOH, Benzil, 60°C, xx. THF, NBS, 0°C.

Scheme 1. Synthetic routes for monomers.[a]

partly reversible reductions at a scan rate of 100 mV/s.

Materials

2,5-Dibromo-1,6-dimethyl benzene, 2,5-dibromothiophene, and 3-thiophene-carboxaldehyde were obtained from Aldrich Chemical Co. Detailed procedures for the monomer synthesis and spectral data are shown in the Supporting Information.

Synthesis and Characterization of Indenofluorene and Monomers 2–5

The synthetic routes of monomers are outlined in Scheme 1. Indenofluorene was synthesized using 2,5-dibromo-1,6-dimethylbenzene as the starting material following the literature procedure with a good yield 86 %.[22] Bis(2-iodo-3-thienyl)methanol, bis(2-iodo-3-thienyl) ketone, and 4*H*-cyclopenta [2,1-b:3,4-b′]dithiophen-4-one are intermediates to synthesize monomers **2–3**. They were synthesized using 3-bromothiophene as the starting material following the literature method.[25] The bis(2-iodo-3-thienyl)ketone was converted to bis (2-iodo-3-thienyl)-4,4-ethylenedioxy by the azeotropic method[8] using benzene and *p*-toluenesulphonic acid in 71% yield, then further reacted to 4,4-ethylenedioxy-4*H*-cyclopenta[2,1-b:3,4-b′]dithiophene by Ullmann coupling reaction[23] using Cu powder and DMF in 93% yield. The 4,4-ethylenedioxy-4*H*-cyclopenta[2,1-b:3,4-b′]dithiophene can also be obtained by reacting 4*H*-cyclopenta[2,1-b:3,4-b′]dithiophen-4-one with ethylene glycol, but with a lower yield of 65%. Monomer 2,6-dibromo-4,4-ethylenedioxy-4*H*-cyclopenta[2,1-b:3,4-b′]dithiophene (**2**) was synthesized by direct bromination of 4,4-ethylenedioxy-4*H*-cyclopenta [2,1-b:3,4-b′]dithiophene with THF and NBS with a yield of 94%. The synthesis of monomer 2,6-dibromo-4,4-propylenedioxy-4*H*-cyclopenta [2,1-b:3,4-b′]dithiophene (**3**) is similar to monomer **2** by only replacing the ethylene glycol to propylene glycol in the reactants and with a comparable yield. The monomer 2,6-dibromo-4*H*-cyclopenta[2,1-b:3,4-b′]dithiophen-4-one (**4**) was synthesized by the direct bromination of 4*H*-cyclopenta[2,1-b:3,4-b′]dithiophen-4-one with THF and NBS with a yield of 93%. 2,3-Diphenyl-5,7-dithiophen-2-yl-thieno[3,4-b]pyrazine was synthesized according to the literature procedure.[21,26] Direct bromination of 2,3-diphenyl-5,7-dithiophen-2-yl-thieno[3,4-b]pyrazine with THF and NBS synthesized the monomer 5,7-bis(5-bromo-thiophen-2-yl)-2,3-diphenyl-thieno[3,4-b] pyrazine (**5**).

General Procedure of Polymerization Through the Suzuki-Coupling Reaction

The polymerization reactions are shown in Scheme 2 and they were based on the palladium catalyzed Suzuki coupling reaction.[27] The general procedure is illustrated later. To a 1:1 molar mixture of 11,11,12,12-tetrahexylindenofluorene-2,7-bis(trimethylene boronate), a dibrominated compound of thiophene derivatives and tetrakis(triphenyl-phosphine) palladium(0) [$Pd(PPh_3)_4$] (1 mol %) was added into a degassed mixture of toluene [(monomer) = 0.1 M] and 2 M potassium carbonate aqueous solution (3:2 in volume). The mixture was vigorously stirred and refluxed at 115°C for 48 h under the protection of nitrogen. After cooling, the mixture was poured into the stirred mixture of methanol and deionized water (10:1). A fibrous solid was obtained by filtration. The solid was redissolved in $CHCl_3$, washed with water three times to remove total alkali solution, dried over anhydrous $MgSO_4$ and evaporated. The residue was dissolved in a minimum volume of $CHCl_3$ and poured into 10 times volume of stirred methanol. The mixture was stirred at room temperature for 2 h, filtered and dried under reduced pressure at room temperature. Yields: 71–93%.

Poly-{2,6-(4,4-ethylenedioxy-4*H*-cyclopenta [2,1-b:3,4-b′]dithiophene)-2,6-(11,11,12,12-tetrahexylindenofluorene)}, P1

Pinkish green powder (Yield 93%). ^{1}H NMR ($CDCl_3$, 400 MHz, ppm): δ 7.75–7.62 (m, 2H), 7.60–7.50 (m, 6H), 7.29 (s, 2H), 4.42 (s, 4H), 2.04 (brt, 8H), 1.11–0.90 (m, 24H), 0.77–0.65 (m, 20H). ^{13}C NMR ($CDCl_3$, 100 MHz, ppm): δ 152.05, 150.47, 147.40, 141.17, 140.26, 137.94, 133.12, 124.57, 124.21, 119.94, 119.49, 117.13, 113.93, 108.06, 65.46, 54.90, 40.74, 31.51, 29.69, 23.75, 22.52, 13.96.

Poly-{2,6-(4,4-propylenedioxy-4*H*-cyclopenta [2,1-b:3,4-b′]dithiophene)-2,6-(11,11,12,12-tetrahexylindenofluorene)}, P2

Brownish black powder (Yield 91%). ^{1}H NMR ($CDCl_3$, 400 MHz, ppm): δ 7.78–7.63 (m, 2H), 7.62–7.55 (m, 6H), 7.54 (brs, 2H), 4.39 (s, 4H), 2.09–1.98 (m, 10H), 1.27–0.99 (m, 24H), 0.78–

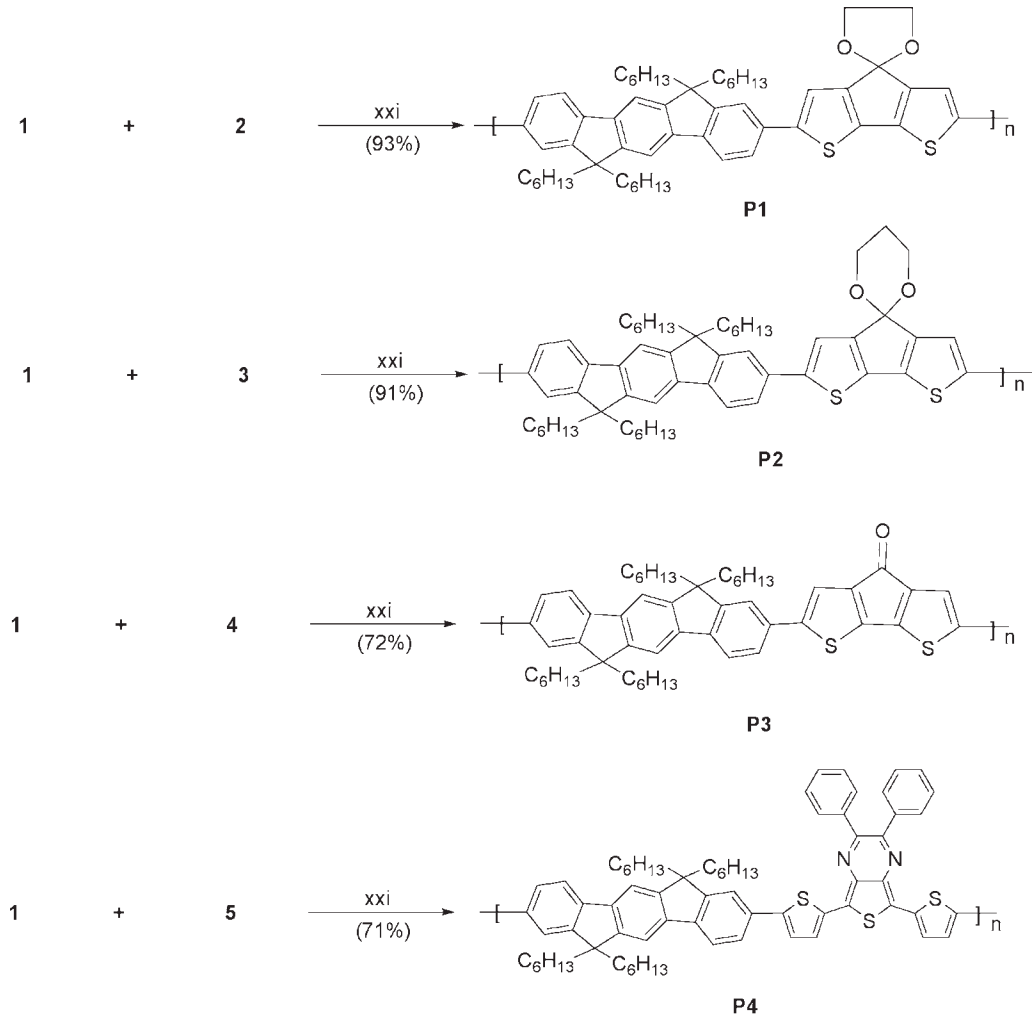

[a]Reagents and Conditions: xxi. $[(PPh_3)_4]Pd(0)$ (1.0 Mol %), Toluene/ 2M K_2CO_3 (3:2), Reflux, 115°C, 48h

Scheme 2. Synthetic routes for polymers.[a]

0.68 (m, 20H). ^{13}C NMR ($CDCl_3$, 100 MHz, ppm): δ 152.05, 150.44, 149.99, 146.66, 141.17, 140.24, 137.28, 133.06, 124.22, 119.94, 119.50, 118.46, 113.90, 101.87, 63.35, 54.90, 40.75, 31.52, 30.91, 29.70, 23.74, 22.53, 13.98.

Poly-{2,6-(4*H*-cyclopenta[2,1-b:3,4-b′] dithiophen-4-one)-2,6-(11,11,12,12-tetrahexyl-indenofluorene)}, P3

Black powder (Yield 72%). IR (KBr) 2926, 2858, 1710, 1448, 1265, 1174, 1026, 822 cm^{-1}. ^1H NMR ($CDCl_3$, 400 MHz, ppm): δ 7.75–7.71 (m, 2H), 7.61–7.46 (m, 6H), 7.30 (brs, 2H), 2.02 (brt, 8H), 1.11–0.90 (m, 24H), 0.77–0.62 (m, 20H). ^{13}C NMR ($CDCl_3$, 100 MHz, ppm): δ 183.56, 152.24, 150.61, 148.40, 147.61, 142.39, 141.69, 140.24, 132.23, 124.17, 120.13, 119.41, 116.99, 114.10, 54.96, 40.67, 31.52, 29.68, 23.77, 22.53, 13.99.

Poly-{5,7-bis(5-thiophen-2-yl)-2,3-diphenyl-thieno[3,4-b]pyrazine)-2,6-(11,11,12,12-tetrahexy-lindenofluorene)}, P4

Deep green powder (Yield 71%) ^1H NMR ($CDCl_3$, 400 MHz, ppm): δ 7.82–7.45 (m, 14H), 7.40–7.33 (m, 8H), 2.09–1.93 (m, 8H), 1.08–0.96 (m, 24H), 0.78–0.60 (m, 20H); ^{13}C NMR ($CDCl_3$, 100 MHz, ppm): δ 152.86, 152.61, 150.53, 150.18, 138.74, 138.53, 132.79, 132.40, 132.15, 132.07, 131.64, 130.16, 129.33, 129.18, 128.25, 128.19, 122.95, 119.95, 115.74, 113.96, 54.81, 40.65, 31.50, 29.69, 23.70, 22.51, 13.96.

Computational Details

Molecular orbital calculations are performed as a independent examination for the electronic and optical properties of the polymers. Polymers with

Table 1. Number Average (M_n), Weight Average (M_w) Molecular Weight, Polydispersity Index and Thermal Properties of **P1–P4**

Polymer	M_n	M_w	PDI (M_w/M_n)	T_g (°C)	T_m (°C)	T_d (°C)
P1	2,982	6,133	2.05	114	N/A	292
P1-F[a]	3,981	5,833	1.46	–	–	–
P2	4,369	9,397	2.15	N/A	N/A	311
P2-F[a]	3,495	4,789	1.37	–	–	–
P3	3,897	6,870	1.77	N/A	159	301
P3-F[a]	3,643	4,741	1.30	–	–	–
P4	5,027	8,319	1.65	78	138	289

[a] Data were retrieved from our previous works (ref. 16).

specified degree of polymerization (1 to 4) were created using the Gaussview program.[28] Note that indenofluorene instead of 11,11,12,12-tetrahexylindenofluorene was used in the calculation to avoid the expensive computation demand (We have found previously that the alkyl side chain does not have a significant effect on the electron density distribution).[16,29] The initial geometry of the polymers was optimized via energy minimization using density functional theory (DFT) at the B3LYP3,4 level with 6–31g* basis sets. We have examined the energy second derivatives (NIMAG = 0) to ensure that a stable minimum-energy state were achieved. Optical transition properties such as the oscillator strength and electronic transition energy were obtained from ZINDO calculations.[30,31]

RESULTS AND DISCUSSION

Synthesis and Characterization of Polymers P1-P4

All the polymers were readily soluble in common organic solvents such as THF, chloroform, toluene and xylene. The number average molecular weight (M_n), weight average molecular weight (M_w), and polydispersity index (M_w/M_n) of these four polymers are given in Table 1. The chemical structures of the monomers and polymers were confirmed by ^{1}H NMR, ^{13}C NMR, and FTIR spectra. The major signal of ^{1}H NMR spectra of **P1**-**P3** at δ 7.29, δ 7.54, and δ 7.30 can be assigned to the proton at position 3 on the cyclopentadithiophene ring. The specific peak of ^{1}H NMR of **P1** at δ 4.42 can be assigned to the four ethylenedioxy protons at position 4 and the peaks at δ 4.39 and δ 2.07 of **P2** can be assigned to the six propylenedioxy protons at position 4 on the cyclopentadithiophene ring. The ^{13}C NMR signal of **P3** at δ 183.56 can be assigned to the carbon at position 4 keto group (C=O) on the cyclopentadithiophene ring. The FTIR spectrum of **P3** film showed a strong band at 1710 cm^{-1} attributed to the carbonyl group (C=O stretching mode). The major signal of ^{1}H NMR spectra of **P4** at δ 7.40–7.33 can be assigned to the protons on the thiophene rings. The ^{13}C NMR signal of **P4** at δ 152.86 can be assigned to imine group (N=C) on the pyrazine ring. The π electrons can be easily delocalized in the polymer chain as compared with its corresponding monomer so spectra of polymers are slightly shifted to downfield.

Thermal Stability

The thermal stability of the copolymers under nitrogen was determined by thermogravimetric analysis (TGA), and their phase transition behaviors were evaluated using differential scanning calorimetry (DSC). Table 1 lists the glass transition temperatures (T_g), the melting temperatures (T_m), and the decomposition temperatures (T_d) of the polymers. All four polymers showed excellent thermal stability with decomposition temperature (5% weight loss, measured by TGA analysis, 10 °C/min) higher than 289 °C. **P1** and **P2** had similar chemical structures; however, T_d of **P1** is lower than that of **P2** by 20 °C, which might be attributed to the more high molecular weight contents in **P2** as suggested by the larger M_w obtained from GPC. **P4** has the lowest T_d, which probably due to the presence of imine group, a less thermal stable bonding. **P3** and **P4** had distinctive melting points while **P1** and **P2** did not have clear T_m, indicating **P3** and **P4** had better crystallinility than **P1** and **P2** had. The difference could result from the variation in the chemical structure: the smaller and polar ketone (—C=0) side chain of **P3** and the planar structure of **P4**

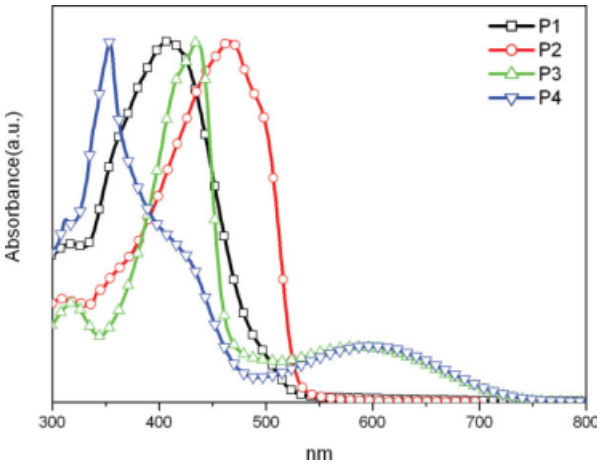

Figure 1. UV-visible absorption spectra of **P1**, **P2**, **P3**, and **P4** in THF solution (ca. 1.67×10^{-5} wt %) at room temperature. [Color figure can be viewed in the online issue, which is available at www.interscience.wiley.com.]

are helpful for crystallization, while the bulky side substituents of **P1** and **P2** are disadvantageous for crystallization.

Optical Properties

The UV-vis absorption and PL spectra of copolymers **P1**-**P4** in THF are shown in Figures 1 and 2 respectively. We have used the onset point of absorption spectra of **P1**-**P4** thin films to estimate the band gap (E_g) of the polymers (see Figure 3). Among these four polymers, the wavelength of the maximum absorption for **P1** and **P2** were more red, which could be attributed to the spiro

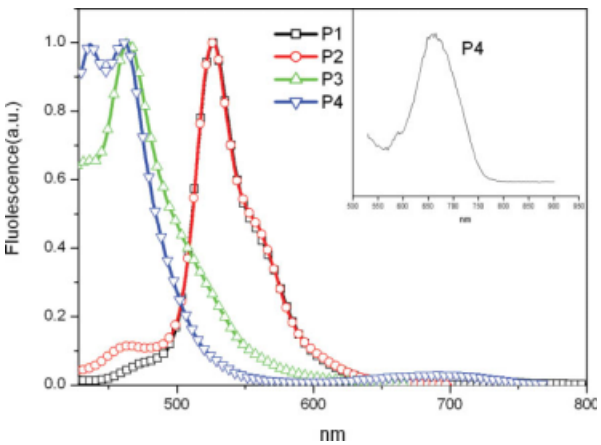

Figure 2. PL spectra of **P1**, **P2**, **P3**, and **P4** in THF solution (ca. 1.67×10^{-5} wt %) at room temperature. Inset shows the weak emission of **P4** in longer range. [Color figure can be viewed in the online issue, which is available at www.interscience.wiley.com.]

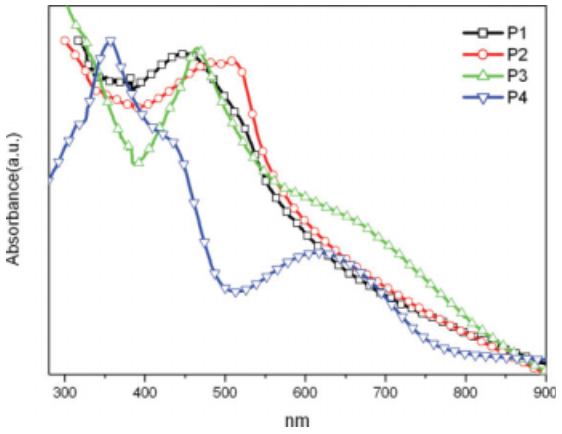

Figure 3. UV-visible absorption spectra of the thin film of **P1**, **P2**, **P3**, and **P4** coated onto fused quartz plate. [Color figure can be viewed in the online issue, which is available at www.interscience.wiley.com.]

connection of the 4,4-ethylenedioxy and 4,4-propylenedioxy groups with the conjugated polymer backbone so that the lone pairs of the oxygen atoms might have certain orbital interactions with the π-electrons of the polymer backbone. Such kind of orbital interactions enables the oxygen atoms serve as electron donating groups to effectively lower the HOMO and thus to reduce the band gap.[32] The absorption of **P2** is slightly red shifted than the absorption of **P1**, which might associate with the more high molecular weight contents of **P2**. In contrast, the absorption maxima for **P3** and **P4** are blue shifted along with a shoulder (**P3**) or weak band (**P4**) in the red edge. Apparently, the $S_0 \rightarrow S_1$ transition becomes less allowed. These photophysical behaviors of **P3** are reminiscent of the *meta* conjugation effect observed for aminostilbenes.[33] In other words, the electronic interaction between the π-substitutents, carbonyl groups, and the π-conjugated polymer backbone resembles the case of *meta*-phenylene bridged subunits. The weak fluorescence of **P3** (Table 2) is also consistent with the forbidden nature of optical transition between S_0 and S_1. For **P4**, the presence of a shoulder in the red edge of its UV-vis absorption spectrum might associate with the low band gap thiophene-pyrazinethiophene-thiophene (T-TP-T) unit. Fluorene based copolymers containing similar T-TP-T units reported in the literatures also exhibited bimodal UV-vis absorption.[34–36]

The UV-vis absorption and PL spectra of copolymers **P1**-**P4** in THF are shown in Figures 1 and 2 respectively. Table 2 also lists the absorption maxima of the four polymers in solid state.

Table 2. Optical Properties of **P1–P4**

Polymer	UV-vis in THF Soln λ max (nm)	PL in THF Soln λ max (nm)	Φ_{fl}	UV-vis in Films λ max (nm)	PL in Films λ max (nm)	E_g (eV)
P1	442	527	0.38	461	548	1.89
P1-F[a]	469	532	0.41	467	554	2.39
P2	466	526	0.36	479,508	571	2.10
P2-F[a]	472	532	0.42	484	564	2.30
P3	435,584	464	<0.01	464,679	512	1.5
P3-F[a]	394,586	508	<0.01	395,589	508	2.59,1.91
P4	354,599	436,462,691[c]	0.02	357,614	498,722	1.6
P4-F[b]	–	–	–	~400,620	–	–

[a] Data were retrieved from our previous works (ref. 16).
[b] Data were retrieved from the UV-vis absorption spectrum in ref. 34.
[c] Data was retrieved from inset in Figure 2.

The comparison between the UV-vis absorption spectrum in solution and those in solid state is discussed as followings. The position of absorption maximum showed only slight shift for **P1** and **P2**. The result could be attributed to the bulky, out of plane ethylenedioxy and propylenedioxy substituents preventing the well-ordered stacking of main chains. The UV-vis absorption of **P3** exhibited a notable red-shift (~30 nm) and an increasing red shoulder in solid state. This observation might associate with the absence of bulky substituents and the strong dipole-dipole interaction between carbonyl groups to assist interchain stacking. For **P4**, the absorption maxima exhibited trivial shifts yet the strength of the red shoulder increased, which probably due to the interchain stacking in solid state. However, the two side phenyl rings are not coplanar with the main chain and thus the interchain stacking of **P4** might not as well organized as that of **P3** to generate a significant red shift. As for PL spectrum, all polymers exhibited red shifts in thin film as expected. It's noted that PL of **P4** in solid state showed a significantly suppress in short wavelength emission and a major emission in long wavelengths, possibly due to the energy transfer from indenofluorene unit to the TP derivatives (see Figure 4).

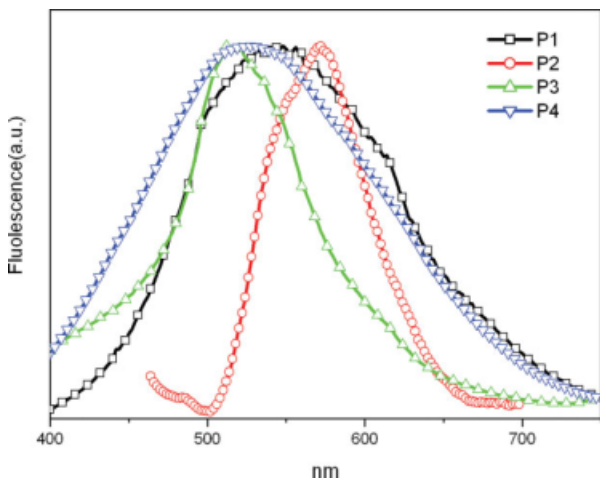

Figure 4. PL spectra of the thin film of **P1**, **P2**, **P3**, and **P4** coated onto fused quartz plate. [Color figure can be viewed in the online issue, which is available at www.interscience.wiley.com.]

Table 3. HOMO-LUMO Gaps (ΔH-L) and $S_0 \rightarrow S_1$ Electronic Transition Energy (E_{abs}) for Different Lengths of **P1–P4** at the B3LYP/6-31G* Optimized Geometry

	P1		**P2**	
n	ΔH-L (eV)	E_{abs}(eV)	ΔH-L (eV)	E_{abs}(eV)
1	3.24	2.69	3.25	2.7
2	2.81	2.42	2.82	2.43
3	2.70	2.38	2.71	2.38
4	2.65	2.35	2.65	2.36
∞	2.59	2.34	2.52	2.33
E_g(exp)[a]	1.88/1.89		2.03/2.10	
	P3		**P4**	
n	ΔH-L (eV)	E_{abs} (eV)	ΔH-L (eV)	E_{abs} (eV)
1	2.65	1.89	2.13	1.79
2	2.39	1.75	1.95	1.68
3	2.31	1.73	1.90	1.65
4	2.28	1.72	1.88	1.64
∞	2.23	1.72	1.85	1.63
E_g(exp)[a]	2.04/1.50		1.93/1.60	

[a] Experimentally determined band gap (Electrochemical/Optical) as shown in Tables 2 and 6.

Table 4. Electronic Transition Data from ZINDO Calculation for Different Lengths of **P1**(4) to **P4**(4) at the B3LYP/6-31G* Optimized Geometry

Copolymer (n)[a]	Electronic Transition[b]	E_{abs} (eV)	f[c]	Main Configurations[b]
P1(4)	**$S_0 \rightarrow S_1$**	**2.35(526)**	**4.63**	**HOMO→LUMO(0.40)**
				HOMO-2→LUMO+3(0.32)
				HOMO-1→LUMO+2(0.31)
	$S_0 \rightarrow S_8$	***3.51(353)***	***1.33***	***HOMO→LUMO+7(0.21)***
				HOMO-3→LUMO+4(0.20)
				HOMO-7→LUMO(0.17)
	$S_0 \rightarrow S_4$	2.70(459)	0.65	
P2(4)	**$S_0 \rightarrow S_1$**	**2.36(525)**	**4.65**	**HOMO→LUMO(0.40)**
				HOMO-2→LUMO+3(0.31)
				HOMO-1→LUMO+2(0.31)
	$S_0 \rightarrow S_8$	***3.51(353)***	***1.47***	***HOMO→LUMO+7(0.21)***
				HOMO-3→LUMO+4(0.20)
				HOMO-7→LUMO(0.17)
	$S_0 \rightarrow S_4$	2.69(460)	0.64	
P3(4)	**$S_0 \rightarrow S_9$**	**3.07(404)**	**4.96**	**HOMO→LUMO+6(0.32)**
				HOMO-2→LUMO+10(0.19)
				HOMO-1→LUMO+5(0.19)
	$S_0 \rightarrow S_1$	***1.72(719)***	***1.28***	***HOMO→LUMO(0.35)***
				HOMO-2→LUMO+2(0.30
				HOMO-1→LUMO+1(0.25)
	$S_0 \rightarrow S_{10}$	3.13(396)	0.70	
P4(4)	**$S_0 \rightarrow S_1$**	**1.64(757)**	**3.31**	**HOMO→LUMO(0.41)**
				HOMO-2→LUMO+2(0.38)
				HOMO-1→LUMO+1(0.33)
	$S_0 \rightarrow S_5$	***2.69(461)***	***1.88***	***HOMO→LUMO+6(0.31)***
				HOMO-2→LUMO+10(0.29)
				HOMO→LUMO+15(0.13)
	$S_0 \rightarrow S_{21}$	3.42(362)	1.34	

[a] Number in parenthesis indicates the chain length n used in the calculation.
[b] Excitation with the largest value of oscillator strength are underlined and that with the second largest values are in italic.
[c] Oscillator strength.

The experimental observations are generally in consistent with the results from quantum mechanical calculations. Listed in Table 3 are the HOMO-LUMO energy gaps (ΔH-L = E_{LUMO}-E_{HOMO}) and the $S_0 \rightarrow S_1$ transition (absorption) gaps (E_{abs}) for **P1** to **P4** with the degree of polymerization (n) varying from 1 to 4. These values are linearly extrapolated to the infinite chain lengths. For **P3** the electronic transitions with the second largest oscillator strength (corresponding to $S_0 \rightarrow S_1$ transitions as explained later) are also given in the parenthesis. It can be seen that the variation of calculated band gaps (ΔH-L) with changing substituent on thiophene derivatives are in good agreement with experimental measurement, i.e., **P3** and **P4** exhibit a lower band gap (the red-shift shoulders in Fig. 1) compared with **P1** and **P2**.

The detailed electronic transitions, including excitation energies, oscillator strength, and configurations for the first two main electronic transitions of **P1** to **P4** (with the degree of polymerization $n = 4$), are presented in Table 4. The calculated excitation energies with the largest oscillator strength correspond to λ_{max} in UV-vis absorption spectrum. For **P1**, **P2**, and **P4**, largest value of oscillator strength is observed from $S_0 \rightarrow S_1$ transition. However, for **P3** electronic transitions from S_0 to a higher excited state become the major transition, whereas the $S_0 \rightarrow S_1$ transition shows the second largest oscillator strength. These results are in agreement with the blue shift in λ_{max} and a shoulder on the red edge in UV-vis absorption spectrum.

It is interesting to note that the blue shift in UV-vis absorption spectrum observed

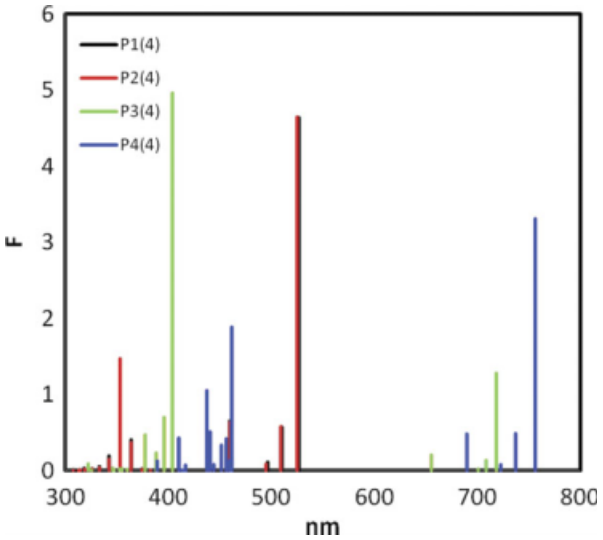

Figure 5. Simulated UV-visible Absorption Spectra by ZINDO Calculation.

experimentally for **P4** may be fundamentally different from that for **P3**. Figure 5 shows the calculated absorption spectrum for **P1(4)** to **P4(4)**. Unlike **P1(4)** and **P2(4)**, whose major absorption bands locate below 550 nm, **P3(4)** and **P4(4)** both display additional absorption bands around 700 nm. While $S_0 \rightarrow S_1$ ($\sim$700 nm) is the transition with a largest oscillator strength for **P4(4)**, there are more electronic transitions allowed around 400–500 nm. This may explain the blue shift observed in the experimental UV-vis spectra. However, the strength of the absorption around 700 nm observed experimentally is much weaker than that around 400–500 nm, which is contradictory to the simulation result stating that the $S_0 \rightarrow S_1$ ($\sim$700 nm) is the major transition.

The differences in electronic transition in **P1** to **P4** can also be understood from their difference in molecular orbital distribution. From Figure 6, the electron density of HOMO and LUMO of **P1** and **P2** are spread over the whole backbone. However, the introduction of electron-withdrawing groups of carbonyl (**P3**) and pyrazine (**P4**) results in localized charge density of LUMO on thiophene derivatives. The higher degree of orbital overlap between HOMO and LUMO implies a stronger electronic transition between HOMO and LUMO.[37] On the contrary, the less orbital overlap between HOMO and LUMO leads to a weaker $S_0 \rightarrow S_1$ electronic transition. These results are consistent with the ZINDO calculations given in Table 4. Combining the spatial distribution of molecular obitals with ZINDO calculations, we

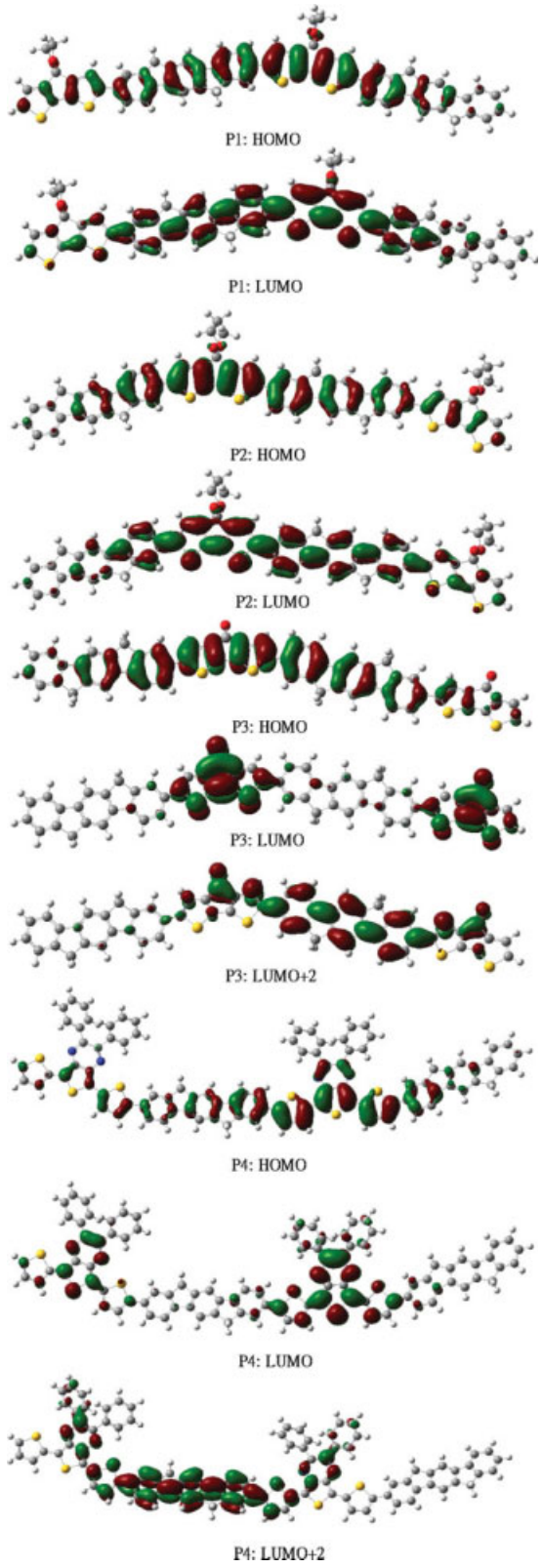

Figure 6. Molecular orbitals of **P1** to **P4** with a chain length $n = 2$.

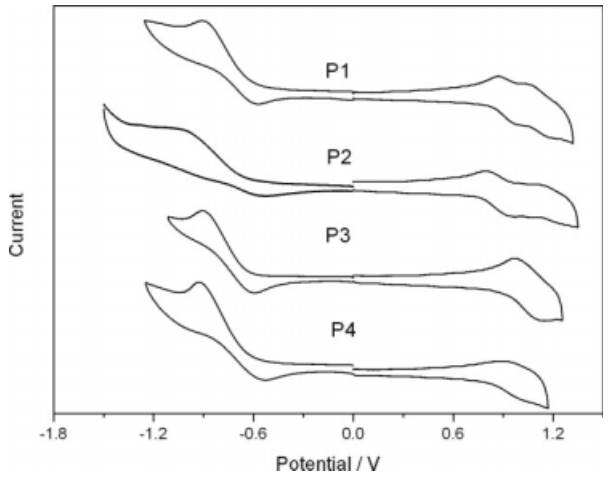

Figure 7. Cyclic voltammograms of the electrochemical oxidation and reduction of copolymers **P1**, **P2**, **P3**, and **P4** in 0.05 M $TBAPF_6$ in CH_2Cl_2 and THF at a sweep rate of 100 mV/s.

can conclude that the weak absorption band (~700 nm) for **P3** and **P4** are mainly attributed to the interaction between HOMO orbital on the overall backbone and LUMO orbital on thiophene derivatives. In addition, the interaction between HOMO and LUMO+2 in Figure 6 play an important role in the blue shift of absorption maxima for **P3** and **P4**.

To understand the effect of using indenofluorene to replace fluorene, we would like to compare the properties of similar copolymers having the same cyclopentadithiophene derivatives. Table 1 and Table 2 respectively list the chemical, thermal properties as well as the electronic and optical properties of fluorene containing copolymers.[16] **Pn-F** (n = 1–4) is denoted as the copolymer comprised of fluorene and the same cyclopentadithiophene derivatives in **Pn** (n = 1–4). It's noticed that the polydispersities of **Pn** were broader than the corresponding **Pn-F**, which might indicate the copolymerization of indenofluorene was more difficult to control. For **P1/P1-F** and **P2/P2-F**, the copolymers containing indenofluorene showed slight blue shifts in UV-vis absorptions both in solution and in solid state. However, in comparison with **P3-F**, **P3** showed significant red shifts both in solution and in solid state. Moreover, the absorption spectrum of **P3-F** in solution was very similar to that in thin film; while the absorption of **P3** in solid state exhibited a notable red shift corresponding to that in solution. The above divergent observations suggest that the incorporation of indenofluorene might result in complicated effects on the electronic and optical properties. Optical red shifts in the absorption spectrum through the elongation of conjugation lengths cannot be always expected. The red shift in **P3** might be attributed to a better steric matching between indenofluorene and monomer **4** leading to a more organized packing. For the comparison of **P4** and **P4-F**, the absorption maxima of **P4** blue-shifted by ~50 nm and the shoulder of the absorption spectrum at long wavelengths of **P4** was suppressed. Nevertheless, the solubility of **P4-F** was very poor and its molecular weight could not be determined from GPC according to the literature (where **P4-F** was denoted as APFO-Green2)[34] while **P4** showed much improved solubility and GPC was tolerable for molecular weight measurement. In summary, indenofluorene might not be an effective moiety on the corresponding copolymers toward light harvesting; however, it did enhance the solubility.

Electrochemical Properties

Cyclic voltammetry (CV) experiments were conducted to probe the electrochemical properties of **P1**-**P4**. The voltammograms and the onset potentials of oxidation ($E_{onset,ox}$) and reduction ($E_{onset,red}$) are shown in Figure 7 and Table 5, respectively. All measurements were calibrated using ferrocene (Fc) value of +0.32 eV as the standard.[38] The HOMO and LUMO and thus the electrochemical band gaps, $E_g = (E_{LUMO} - E_{HOMO})$,[39,40] could be estimated (Table 5) according to the empirical relationship proposed by de Leeuw et al. [eq. (1)][41]:

$$\begin{aligned} I_p(\text{HOMO}) &= -(E_{onset,ox} + 4.39)(\text{eV}), \\ E_a(\text{LUMO}) &= -(E_{onset,red} + 4.39)(\text{eV}) \end{aligned} \quad (1)$$

The electrochemical band gaps of P1 and P2 are in a good agreement with the optical band gaps; however, those of P3 and P4 are larger than

Table 5. Electrochemical Properties and Energy Levels of **P1–P4**

Polymer	$E_{onset,oxd}$ (eV)	$E_{onset,red}$ (eV)	HOMO (eV)	LUMO (eV)	E_g (eV)
P1	0.97	−0.91	5.36	3.48	1.88
P2	1.01	−1.02	5.40	3.25	2.03
P3	1.14	−0.90	5.53	3.49	2.04
P4	1.01	−0.92	5.40	3.47	1.93

the corresponding optical band gaps (see Table 2). The discrepancies for P3 and P4 might associate with the insensitivity of cyclic voltammetry measurement on the weak $S_0 \rightarrow S_1$ transition.

CONCLUSION

We have demonstrated an efficient method to synthesize a new series of indenofluorene based copolymers. The polymers prepared showed good solubility in common organic solvents. Efficient absorption spectra tuning are demonstrated by changing the substitutes of the thiophene based derivatives. Some of the polymers behavior that resembles the *meta* conjugation effect for π-substituents at the bridge position might prove of values in designing new materials for the fabrication of polymer solar cells. These copolymers are low band gap with low PL and thus they might be good candidates as the photoactive materials in solar cells.

We thank the National Science Council of Taiwan (NSC 95-2120-M-002-012) and US Air Force (AOARD-07-4014) supporting this research.

REFERENCES AND NOTES

1. Shaheen, S. E.; Brabec, C. J.; Sariciftci, N. S.; Padinger, F.; Fromherz, T.; Hummelen, J. C. Appl Phys Lett 2001, 78, 841–843.
2. Zeng, T.-W.; Lin, Y.-Y.; Chen, C.-W.; Su, W.-F.; Chen, C.-H.; Liou, S.-C.; Huang, H.-Y. Nanotechnology 2006, 17, 5387–5392.
3. Zhou, E.; Tan, Z.; He, Y. J.; Yang, C. H.; Li, Y. F. J Polym Sci Part A: Polym Chem 2007, 45, 629–638.
4. Shin, W. S.; Kim, S. C.; Lee, S. J.; Jeon, H. S.; Kim, M. K.; Naidu, B. V. K.; Jin, S.-H.; Lee, J. K.; Lee, J. W.; Gal, Y. S. J Polym Sci Part A: Polym Chem 2007, 45, 1394–1402.
5. Huo, L.; He, C.; Han, M. F.; Zhou, E.; Li, Y. F. J Polym Sci Part A: Polym Chem 2007, 45, 3861–3871.
6. Tang, W. H.; Kietzke, T.; Vemulamada, P.; Chen, Z. K. J Polym Sci Part A: Polym Chem 2007, 45, 5226–5276.
7. Zhao, C. C.; Chen, X. H.; Zhang, Y.; Ng, M. K. J Polym Sci Part A: Polym Chem 2008, 46, 2680–2688.
8. Huo, L.; Tan, Z.; Wang, X.; Zhou, Y.; Han, M. F.; Li, Y. F. J Polym Sci Part A: Polym Chem 2008, 46, 4038–4079.
9. Li, K. C.; Hsu, Y. C.; Lin, J. T.; Yang, C. C.; Wei, K. H.; Lin, H. C. J Polym Sci Part A: Polym Chem 2008, 46, 4285–4304.
10. Park, J. S.; Ryu, T. I.; Song, M. K.; Yoon, K. J.; Lee, M. J.; Shin, I. A.; Lee, G. D.; Lee, J. W.; Gal, Y. S.; Jin, S. H. J Polym Sci Part A: Polym Chem 2008, 46, 6175–6184.
11. Kastner, J.; Kuzmany, H.; Vegh, D.; Landl, M.; Cuff, L.; Kertesz, M. Macromolecules 1995, 28, 2922–2929.
12. Roncali, J. Chem Rev 1997, 97, 173–206.
13. Wienk, M. M.; Struijk, M. P.; Janssen, R. A. J. Chem Phys Lett 2006, 422, 488–491.
14. Wienk, M. M.; Turbiez, M. G. R.; Struijk, M. P.; Fonrodona, M.; Janssen, R. A. J. Appl Phys Lett 2006, 88, 153511–153513.
15. Coppo, P.; Cupertino, D. C.; Yeates, S. G.; Turner, M. L. J. Mater Chem 2002, 12, 2597–2599.
16. Pal, B.; Yen, W.-C.; Yang, J.-S.; Chao, C.-Y.; Hung, Y.-C.; Lin, S.-T.; Chuang, C.-H.; Chen, C.-W.; Su, W.-F. Macromolecules 2008, 41, 6664–6671.
17. Fusalba, F.; Ei Mehdi, N.; Breau, L.; Belanger, D. Chem Mater 1999, 11, 2743–2753.
18. Kozaki, M.; Tanaka, S.; Yamashita, Y. J. Org Chem 1994, 59, 442–450.
19. Berlin, A.; Zotti, G.; Zecchin, S.; Schiavon, G.; Vercelli, B.; Zanelli, A. Chem Mater 2004, 16, 3667–3676.
20. Coppo, P.; Turner, M. L. J. Mater Chem 2005, 15, 1123–1133.
21. Zhang, F.; Perzon, E.; Wang, X.; Mammo, W.; Andersson, M. R.; Inganas, O. Adv Func Mater 2005, 15, 745–750.
22. Merlet, S.; Birau, M.; Wang, Z.-Y. Org Lett 2002, 4, 2157–2159.
23. Marsitzky, D.; Scott, J. C.; Chen, J. P.; Lee, V. Y.; Miller, R. D.; Setayesh, S.; Muellen, K. Adv Mater 2001, 13, 1096–1099.
24. Hadizad, T.; Zhang, J.; Wang, Z.-Y.; Gorjanc, T. C.; Py, C. Org Lett 2005, 7, 795–797.
25. Brzezinski, J. Z.; Reynolds, J. R. Synthesis 2002, 2002, 1053–1056.
26. Kenning, D. D.; Mitchell, K. A.; Calhoun, T. R.; Funfar, M. R.; Sattler, D. J.; Rasmussen, S. C. J. Org Chem 2002, 67, 9073–9076.
27. Suzuki, A.; Miyaura, N. Chem Rev 1995, 95, 2457–2483.
28. Frisch, M. J. T.; Schlegel, G. W.; Scuseria, G. E.; Robb, M. A.; Cheeseman, J. R.; Montgomery, J. A.; Vreven, T., Jr.; Kudin, K. N.; Burant, J. C.; Millam, J. M.; Iyengar, S. S.; Tomasi, J.; Barone, V.; Mennucci, B.; Cossi, M.; Scalmani, G.; Rega, N.; Petersson, G. A.; Nakatsuji, H.; Hada, M.; Ehara, M.; Toyota, K.; Fukuda, R.; Hasegawa, J.; Ishida, M.; Nakajima, T.; Honda, Y.; Kitao, O.; Nakai, H.; Klene, M.; Li, X.; Knox, J. E.; Hratchian, H. P.; Cross, J. B.; Adamo, C.; Jaramillo, J.; Gomperts, R.; Stratmann, R. E.; Yazyev, O.; Austin, A. J.; Cammi, R.; Pomelli, C.; Ochterski, J. W.; Ayala, P. Y.; Morokuma, K.; Voth, G. A.; Salvador, P.; Dannenberg, J. J.; Zakrzewski, V. G.; Dapprich, S.; Daniels, A. D.; Strain, M. C.; Farkas,

O.; Malick, D. K.; Rabuck, A. D.; Raghavachari, K.; Foresman, J. B.; Ortiz, J. V.; Cui, Q.; Baboul, A. G.; Clifford, S.; Cioslowski, J.; Stefanov, B. B.; Liu, G.; Liashenko, A.; Piskorz, P.; Komaromi, I.; Martin, R. L.; Fox, D. J.; Keith, T.; Al-Laham, M. A.; Peng, C. Y.; Nanayakkara, A.; Challacombe, M.; Gill, P. M. W.; Johnson, B.; Chen, W.; Wong, M. W.; Gonzalez, C.; Pople, J. A. Gaussian 03, Revision C.02; Gaussian, Inc.: Wallingford CT, 2004.

29. Frisch, A.; Nielsen, A. B.; Holder, A. J. Gaussview Users Manual; Gaussian Inc.: 2000.
30. Becke, A. D. J Chem Phys 1993, 98, 5648–5652.
31. Lee, C. T.; Yang, W. T.; Parr, R. G. Phys Rev B 1988, 37, 785–789.
32. Brisset, H.; Thobie-Gautier, C.; Gorgues, A.; Jubault, M.; Roncali, J. J. Chem Soc Chem Commun 1994, 1305–1306.
33. Yang, J.-S.; Liau, K.-L.; Tu, C.-W.; Hwang, C.-Y. J Phys Chem A 2005, 109, 6450–6456.
34. Perzon, E.; Wang, X. J.; Zhang, F. L.; Mammo, W.; Delgado, J. L.; De La Cruz, P.; Inganas, O.; Langa, F.; Andersson, M. R. Synth Met 2005, 154, 53–56.
35. Xia, Y.; Luo, J.; Deng, X.; Li, X.; Li, D.; Zhu, X. Y.; Cao, W. Y. Macromol Chem Phys 2006, 207, 511–520.
36. Lee, W. Y.; Cheng, K.-F.; Wang, T.-F.; Chueh, C.-C.; Chen, W. C.; Tuan, C. S.; Lin, J. L. Macromol Chem Phys 2007, 208, 1919–1927.
37. Clarke, T. M.; Gordon, K. C.; Officer, D. L.; Hall, S. B.; Collis, G. E.; Burrell, A. K. J Phys Chem A 2003, 107, 11505–11516.
38. Pommerehe, J.; Vestweber, H.; Guss, W.; Mahrt, R. F.; Bassler, H.; Porsch, M.; Daub, J. Adv Mater 1995, 7, 55–58.
39. Pei, J.; Yu, W.-L.; Huang, W.; Heeger, A. J. Macromolecules 2000, 33, 2462–2471.
40. Chen, Z.-K.; Huang, W.; Wang, L.-H.; Kang, E.-T.; Chen, B. J.; Lee, C. S.; Lee, S. T. Macromolecules 2000, 33, 9015–9025.
41. De Leeuw, D. M.; Simenon, M. M. J.; Brown, A. R.; Einerhand, R. F. F. Synth Met 1997, 87, 53–59.